Bisperoxovanadium Mediates Neuronal Protection through Inhibition of PTEN and Activation of PI3K/ AKT-mTOR Signaling after Traumatic Spinal Injuries

Chandler L. Walker,[1,2] Xiangbing Wu,[2] Nai-Kui Liu,[2] and Xiao-Ming Xu[2]

Abstract

Although mechanisms involved in progression of cell death in spinal cord injury (SCI) have been studied extensively, few are clear targets for translation to clinical application. One of the best-understood mechanisms of cell survival in SCI is phosphatidylinositol-3-kinase (PI3K)/Akt and associated downstream signaling. Clear therapeutic efficacy of a phosphatase and tensin homologue (PTEN) inhibitor called bisperoxovanadium (bpV) has been shown in SCI, traumatic brain injury, stroke, and other neurological disease models in both neuroprotection and functional recovery. The present study aimed to elucidate mechanistic influences of bpV activity in neuronal survival in *in vitro* and *in vivo* models of SCI. Treatment with 100 nM bpV(pic) reduced cell death in a primary spinal neuron injury model ($p < 0.05$) *in vitro*, and upregulated both Akt and ribosomal protein S6 (pS6) activity ($p < 0.05$) compared with non-treated injured neurons. Pretreatment of spinal neurons with a PI3K inhibitor, LY294002 or mammalian target of rapamycin (mTOR) inhibitor, rapamycin blocked bpV activation of Akt and ribosomal protein S6 activity, respectively. Treatment with bpV increased extracellular signal-related kinase (Erk) activity after scratch injury *in vitro*, and rapamycin reduced influence by bpV on Erk phosphorylation. After a cervical hemicontusive SCI, Akt phosphorylation decreased in total tissue via Western blot analysis ($p < 0.01$) as well as in penumbral ventral horn motor neurons throughout the first week post-injury ($p < 0.05$). Conversely, PTEN activity appeared to increase over this period. As observed *in vitro*, bpV also increased Erk activity post-SCI ($p < 0.05$). Our results suggest that PI3K/Akt signaling is the likely primary mechanism of bpV action in mediating neuroprotection in injured spinal neurons.

Keywords: bisperoxovanadium; bpV; mTOR spinal cord injury; neuroprotection; PTEN

Introduction

ACUTE SPINAL CORD INJURY (SCI) is devastating with an annual incidence of approximately 12,000 cases in the United States alone.[1] As life expectancy increases, as well as the number of patients with SCI, worldwide prevalence approaches approximately 2 million.[1,2] An estimated US $4 billion are spent on medical treatment alone for acute SCI and associated rehabilitative management.[1,3] Despite these staggering numbers, there are still no cures for SCI.

Our knowledge of cellular and pathological responses to injury is incomplete, which hinders effective clinical progress in therapeutic development and application.[4] Exogenous promotion of neuroprotection and recovery using readily available and fast acting therapeutics would be valuable, however, for slowing secondary injury and its destruction of initially spared tissue.[5] Consequently, understanding mechanisms by which such treatments act is as important as identifying the therapies themselves.

Modulating the activity or expression of the phosphatase and tensin homologue, PTEN, promotes axon regeneration,[6–10] and neuroprotection after central nervous system (CNS) injury and neurodegeneration.[11–18] PTEN is a known antagonist of phosphatidylinositol-3-kinase (PI3K), preventing phosphatidylinositol triphosphate (PIP$_3$) from promoting phosphorylation and activation of the prosurvival kinase, Akt. Inhibiting PTEN disinhibits PI3K signaling leading to improved cell survival, tissue sparing, and functional '[11,12,14–16] potentially through reducing delayed destructive processes.

We demonstrated that PTEN expression does not significantly change 24 h post-SCI, although phosphorylated (active) Akt decreases, suggesting that the lipid phosphatase of PTEN activity and the antagonism of PI3K increases within injured tissue after SCI. Thus, our previous evidence supports the hypothesis that PTEN activity promotes cell death after SCI. We identified neurons as potential targets of PTEN inhibition because they expressed PTEN

[1]Department of Biomedical and Applied Sciences, Indiana University School of Dentistry, Indianapolis, Indiana.
[2]Spinal Cord and Brain Injury Research Group, Stark Neurosciences Research Institute, Department of Neurological Surgery and Goodman Campbell Brain and Spine, Indiana University School of Medicine, Indianapolis, Indiana.

before and after injury, and treatment with a potent PTEN inhibitor, dipotassium bisperoxo (picolinato) vanadium (bpV[pic]),[19] induced significant ventral horn neuron survival after cervical hemicontusion SCI.

Although whole tissue protein analysis revealed significant reduction in Akt phosphorylation in the proximity of the injury site one day post-SCI, it is unclear whether this suppression is sustained in surviving spinal neurons after injury. Also, our previous research did not confirm whether bpV acted directly on neurons in promoting their survival after SCI. Further, our results suggested that bpV acted through PI3K/Akt signaling post-injury; however, our findings did not reveal whether bpV operated via this mechanism specifically in neurons.

We therefore designed the present study to assess the extent of the modulation of Akt phosphorylation after SCI to extend our understanding of bpV-mediated neuroprotection and to determine more effectively whether bpV acts on PTEN and PI3K/Akt signaling or other mechanisms in spinal neurons after traumatic injury.

Methods

Schematic diagrams of *in vivo* and *in vitro* experimental designs are shown in Figure 1.

In vitro *experiments*

Primary spinal neuron culture and treatment. Primary spinal cord neurons were obtained from SD rat E15 embryo spinal cords according to an established protocol.[20] In brief, E15 rat spinal cords were isolated and placed in Leibovitz L-15 medium (Gibco, Grand Island, NY). Meninges were carefully removed, the spinal cords were cut into small pieces and dissociated with 0.05% trypsin/ethylenediaminetetraacetic acid (EDTA) for 15–20 min at 37°C and gently triturated. After adhering at 37°C for 30 min to eliminate glial cells and fibroblasts, neurons were plated on poly-L-lysine pre-coated 48-well plates (Corning, Tewksbury, MA).

Neurons were incubated in a humidified atmosphere containing 5% CO_2 at 37°C with Delbecco Modified Eagle Medium +10% heat-inactivated fetal bovine serum +5% heat-inactivated horse serum +2 mM glutamine. After 16 h, the medium was replaced with Neurobasal medium with 2% B27, 1% N2 and 2 mM glutamine (all from Life Technologies, Inc., Grand Island, NY). On day 3 *in vitro*, 5 μM cytosine-β-D-arabinofuranoside (Sigma-Aldrich, St. Louis, MO) was added for 24 h to inhibit glia cell proliferation.

Cells in 48-well plates were cultured with 200 μL medium until experimentation. With this culture protocol, a purity of greater than 87% spinal cord neuron population was obtained by seven days *in vitro* (DIV). All experiments were performed between seven and 10 DIV.

In vitro traumatic neural injury model. Primary spinal neurons were cultured as described. At the time of experimentation, cells were given either a fresh medium change (control) or were mechanically damaged by a monolayer scratch injury model modified from previous studies.[21] In summary, an 18-gauge surgical needle was flattened to increase the surface area of damage, and distinct grid patterns of scratches were performed in either 48-well or six-well culture plates containing 7-10 DIV mixed spinal neuron culture (Fig. S1).

In 48-well plates, used for supernatant collection for cell death assessment, immunolabeling, and imaging, four vertical and three horizontal scratch lines (space 3 mm apart) were made to the neuron monolayer, causing immediate damage to neuron cell bodies and neurites (Fig. S1A). In 6-well plates, used for cell lysate and protein collection, seven vertical and five horizontal scratch lines (all spaced 5 mm apart) were created (Fig. S1B). The needle and scratch designs were determined experimentally for optimal use in producing graded injury over time, and served as a useful and responsive model for experimental treatment with bpV and other signal pathway inhibitors.

To assess graded injury over time, supernatant was collected from 48-well groups at time intervals of 1, 4, 16, and 24 h post-injury, and a cell death assay was performed. Fluorescent nuclear labeling of propidium iodide (PI) was also utilized to confirm changes visually in cell viability, in combination with a cell death assay, in experiments testing neuroprotective effects of bpV after scratch injury. The scratch method induced a primary mechanical injury to neurons/neurites at the injury site and caused a subsequent spread of damage to adjacent neurons distal to the scratch lines over time.
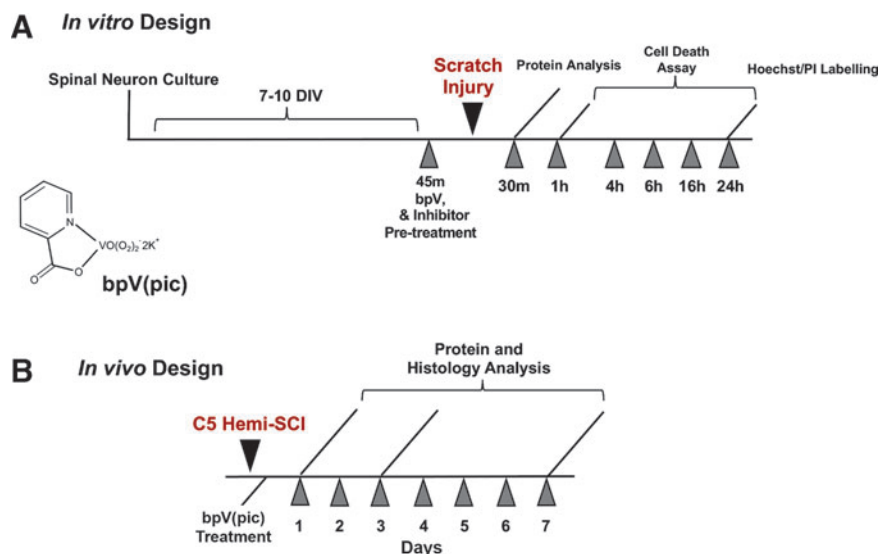

FIG. 1. *In vitro* and *in vivo* experimental design and timeline. PI, propidium iodide; C5 Hemi-SCI, cervical level 5 hemicontusion spinal cord injury; bpV(pic), dipotassium bisperoxo (picolinato) vanadium.

Assessment of bpV treatment effects on spinal neurons. In wells selected for experimental treatment, a 45 min pre-treatment with experimentally determined doses of 100 nM PTEN inhibitor bpV(pic) (Enzo Life Sciences, Farmingdale, NY) in 0.9% saline, 20 μM PI3K-inhibitor LY294002, 25 nM mammalian target of rapamycin (mTOR) inhibitor rapamycin (LC Laboratories, Woburn, MA), or combinations of the above were implemented. After pre-treatment, cells were left uninjured or received scratch injuries and were cultured for designated periods depending on the experiment. After experimental treatment, supernatant was collected for cell death assays, and cells were prepared for either Western blot analysis or immunocytochemistry.

PI neuron death labeling. The PI labeling to indicate neuronal death was performed as described previously.[22] In brief, Hoechst 33342 (Sigma-Aldrich) was added to culture wells, and plates were incubated at 37°C and 95% O_2/5% CO_2 for 10 min to label all cell nuclei. Plates were then incubated with PI (Sigma-Aldrich) at room temperature for 15 min to label nuclei of dead cells. After PI incubation, medium was extracted, and cells were washed with 0.01 M phosphate-buffered saline (PBS), followed by a 10 min treatment with 4% paraformaldehyde (PFA) in 0.1 M PBS to fix the cells.

Cells were then washed with PBS and labeled with AlexaFluor 488-conjugated β-III-tubulin primary antibody (EMD Millipore, Billerica, MA) for 1 h in PBS-T for neuron labeling +10% normal goat serum to prevent non-specific antibody binding. Cells were then washed 3×5 min with PBS-T and covered with PBS in the well for imaging.

Cell death assay. To assess the damage and death of cultured spinal neurons, a lactase dehydrogenase (LDH) release assay was performed on the cell culture supernatant per the manufacturer's instructions (Cytotox 96, Promega, Madison, WI). Briefly, 50 μL medium was removed from each well with cultured neurons in a 48-well plate after 24 h injury experiment and transferred to corresponding wells of an empty flat-bottomed 96-well plate. Supplied LDH substrate mix (50 μL) was added to each well, and the plates were left in the dark for 30 min. Afterward, reaction Stop Buffer was added to end LDH enzyme activity, and the plates were read on a plate reader at an absorbance 490 nm. A numerical absorbance value for each well was calculated as a measure of the amount of LDH release by the neurons with and without scratch injury.

Western blotting. Spinal neurons used for protein analysis were cultured on six-well plates as described above. Proteins were prepared for Western blot analysis according to previously published methods.[11,23] In brief, approximately 1.5×10^6 cells/well were lysed in RIPA Lysis Buffer (25 mM Tris-HCl [pH 7.6], 150 mM NaCl, 1% NP-40, 1% sodium deoxycholate, 0.1% SDS +0.5 M EDTA, and 1% Halt inhibitor), homogenized, and left on ice for 15 min. Then, the lysates were centrifuged, supernatants extracted, and protein concentrations were determined using the Bradford method.[24]

Samples were loaded on 8–10% SDS polyacrylamide gels, separated via electrophoresis, and proteins were transferred onto polyvinylidene fluoride (PVDF) membranes. Membranes were blocked with Li-Cor Odyssey blocking buffer (Li-Cor, Lincoln, NE) for 1 h followed by incubation with the following primary antibody overnight at 4°C: polyclonal rabbit anti-phospho Akt (ser 473) (1:1,000), a marker used for assessing PTEN and PI3K activation; monoclonal mouse anti-pan Akt (1:1,500); polyclonal rabbit anti-phospho ribosomal protein S6 (ser 235/236) (1:400); rabbit anti-extracellular signal-related kinase (Erk) (1:1,500); mouse anti-phospho Erk (1:1,000); and mouse anti-β-tubulin (1:1000, Sigma-Aldrich) as a loading control.

Membranes were then washed with PBS-T and incubated with secondary antibody (goat anti-mouse IR Dye800 or goat anti-rabbit IR Dye680 (Rockland Immunochemicals Inc., Gilbertsville, PA) 1 h at room temperature. Membranes were scanned using a LiCor Odyssey infrared scanner and images captured using Image Studio 2.0 software (Li-Cor). Densitometry of specific bands was performed using ImageJ software (National Institutes of Health [NIH], Bethesda, MD).

In vivo *experiments*

Surgical procedures. For investigating acute signaling mechanism changes and bpV effects *in vivo*, adult female Sprague-Dawley rats (SD, 200–250 g, Harlan, Indianapolis, IN) ($n=40$) were maintained under controlled conditions with a 12:12 light:dark cycle with *ad libitum* water and food access. For time course investigation of signaling mechanism changes, a sham surgery group ($n=8$), and animals designated for sacrifice one day ($n=8$), three days ($n=8$), and seven days ($n=8$) post-surgery were established. For animals designated for the acute assessment of bpV treatment effects, two groups were established: control and bpV treatment groups ($n=4$, each).

Before the surgical procedure, animals were anesthetized intraperitoneally (IP) with a ketamine/xylazine cocktail ([87 mg/kg]/[12 mg/kg]) and received laminectomy only (sham operation) or unilateral cervical contusive SCI performed as published previously.[11] In brief, a customized device was used to stabilize the 5th cervical vertebra,[25] and a partial unilateral laminectomy exposed the right side of the cord leaving the dura intact. The MASCIS Impactor[26] (10 g weight, 12.5 mm height) produced a moderate unilateral injury.[27] Sham animals were administered anesthesia and laminectomy surgery, but were excluded from injury.

Animals received 5 mL 0.9% saline subcutaneously for hydration and were observed over a 24 h recovery period in temperature-controlled housing. All animal procedures and surgeries were approved under the Guide for the Care and Use of Laboratory Animals (National Research Council) and the Guidelines of the Indiana University School of Medicine Institutional Animal Care and Use Committee.

bpV treatment post-SCI. After injury, the control rats received an immediate IP injection of 0.9% saline (Vehicle) and the bpV treatment group received an injection of bpV(pic) (Enzo Life Sciences) 400 μg/kg. The rats then received a subsequent injection of Vehicle or bpV 2 h post-SCI and were sacrificed 24 h after the surgical procedure for tissue isolation. Tissue collected from sham operation and one day post-SCI rat groups from the time course study were utilized for comparison.

Western blotting. Tissue protein analysis from *in vivo* experiments followed procedures described previously[11,23] with modification. Briefly, a 10 mm spinal cord segment containing the injury epicenter (5 mm rostral and caudal to the epicenter) was removed for protein extraction from sham rats and animals one, three, and seven days after SCI. Equal protein concentrations from each sample were loaded onto 8–10% polyacrylamide gels, separated by SDS-PAGE, and transferred to a PVDF membrane.

The membranes were immunoblotted with the following primary antibodies: monoclonal mouse-anti PTEN (1:200) (Santa Cruz Biotechnologies, Santa Cruz, CA); rabbit anti-phospho-PTEN (ser 380, 1:500), a marker for the inactive form of PTEN; polyclonal rabbit anti-phospho Akt (ser 473) (1:1,000); monoclonal mouse anti-pan Akt (1:1,500); polyclonal rabbit anti-phospho ribosomal protein S6 (ser 235/236) (1:400); rabbit anti-phospho ser9-glycogen synthase kinase 3β (GSK3β) (1:1000), inhibited form of GSK3β induced by Akt; rabbit anti-Erk (1:1,500); mouse anti-phospho Erk (1:1,000); cleaved caspase 3 (1:500) a marker for apoptotic cell death (Cell Signaling, Inc., Danvers, MA); mouse anti-β-tubulin (1:1000, Sigma-Aldrich) as a loading control.

Membranes were incubated with a secondary goat anti-rabbit or anti-mouse fluorescent IR680 or IR800 secondary antibody (1:10,000; Rockland) and visualized with the Li-Cor Odyssey system and software as described. Quantification of detected bands was performed by densitometry using ImageJ software (NIH).

Histological preparation. Tissue was collected from sham rats and animals one, three, and seven days post-SCI and processed as previously published.[11,23] In brief, a 1 cm segment of cervical cord including the injury epicenter was dissected and sectioned transversely at 20 μm thicknesses on Superfrost Plus slides (Fisher Scientific, Waltham, MA) using a cryostat (Leica Biosystems, Buffalo Grove, IL). Serial sections with an interval of 0.5 mm along the length of the cord were used spanning the entire segment.

A set of slides was stained with cresyl violet/eosin to identify the lesion epicenter and 2 mm rostral and caudal to the epicenter. Adjacent sections in this penumbral region were selected for immunofluorescence labeling to determine the pattern of p-Akt expression in surviving near-lesion neurons and the number of these neurons during the first week post-SCI.

Immunofluorescence double labeling. Immunofluorescence double labeling was performed as described previously.[11,12,23,28] Briefly, sham animals and animals one, three, and seven days after SCI were perfused with 4% paraformaldehyde, and a 1 cm-long spinal segment including the injury epicenter was removed and cryoprotected in 30% sucrose in 0.1 M PBS. Cord segments were sectioned transversely at 20 μm thicknesses, mounted on Superfrost slides, and prepared for immunostaining as described previously.[11]

Tissue sections were incubated with the following primary antibodies: mouse anti-NeuN (1:200, EMD Millipore), a marker for neurons, and rabbit anti-phospho-Akt (ser473) (1:100, Cell Signaling, Inc.). The following day, the sections were incubated with rhodamine-conjugated goat anti-rabbit or fluoroisothiocyanate (FITC)-conjugated anti-mouse fluorescent secondary antibodies (1:200, Jackson ImmunoResearch Lab, West Grove, PA). Sections were coverslip-mounted with Fluoromount G (Southern Biotech, Birmingham, AL). Pre-immune serum was used as a control to confirm antibody specificity. Images were obtained at identical settings with an Olympus BX60 epifluorescent microscope.

Fluorescent intensity of p-Akt in motor neurons 1.5 mm to 2 mm rostral to the epicenter (in the injury penumbra) was performed using ImageJ. This was achieved by converting the images to gray scale, outlining NeuN/p-Akt double labeled neurons of the ventral horn, and measuring the integrated density (ID) of p-Akt labeling of the neurons. Background values were obtained from five identically sized sample areas of tissue adjacent to the quantified neurons, and an average background ID was calculated. The measured neuron ID was divided by the mean background ID to achieve neuron ID signal to background ID ratio values for each neuron.

Approximately 10–20 motor neurons 1.5–2 mm rostral to the epicenter were measured per animal, and the signal/background ratio was averaged for all measurements from each animal, and all animals per group. Ventral horn neurons positive for NeuN labeling in these sections were quantified using a previously published method.[11]

Statistical analysis

A two-sample Student t test was used to determine significance between two groups. Statistical significance between multiple groups was determined using a one-way analysis of variance with *post hoc* analysis. All statistical values were calculated with GraphPad Prism 5.0 software (GraphPad, Inc., La Jolla, CA), with a p value < 0.05 considered statistically significant.

Results

Treatment with bpV reduced damage induced by a traumatic neuron injury in vitro

To confirm bpV-mediated neuroprotection in spinal neurons, we employed an established purified spinal neuron culture protocol.[20] To mimic the traumatic mechanical injury inflicted on spinal neurons and induce extended secondary cell damage as observed after SCI, we used a scratch injury model to inflict trauma to wide paths of neurons and their processes (neurites). The scratch patterns used in 48- and six-well culture plates are shown in Fig. S1; see online supplementary material at www.liebertpub.com. This model caused rapid and continued cell damage, and LDH release from the cells continued to increase to 24 h post-injury (Fig. 2A, $p < 0.01$ vs. control at each time point).

As observed in a contusive SCI model *in vivo*, bpV demonstrated neuroprotective effects on injured primary spinal neurons in culture. Acute LDH release was decreased by100 nM bpV measured 6 h post-injury (Fig. 2B, $p < 0.05$). Corroborating this result, bpV reduced PI positive cells by 24 h post-injury (Fig. 2C) compared with the non-treatment group. At this time, cell death was most evident near the injury site as represented by numerous PI positive cells compared with non-injured cells (Fig. 2C).

Treatment with bpV stimulated activation of Akt and mTOR in injured spinal neurons

On confirmation of protective effects of the compound on spinal neurons, we used the same scratch injury model to determine whether the injury induced changes in Akt and mTOR signaling, and whether bpV had an effect on the PTEN-PI3K/Akt-mTOR signaling pathway in primary spinal neurons. At 30 min after injury, Akt activity significantly decreased by $\sim 20\%$ ($p < 0.01$) (Fig. 3A). Treatment with 100 nM bpV significantly elevated Akt activity (36%) in injured neurons at 30 min post-scratch *in vitro* ($p < 0.001$, Fig. 3A,), and induced a 25% increase in p-S6 activity over injury level ($p < 0.05$, Fig. 3B).

To validate the activity of bpV on PI3K/Akt/mTOR signaling, experiments were carried out using a PI3K inhibitor, LY294002, and an mTOR inhibitor, rapamycin, on injured spinal neurons. When neurons were treated with bpV and LY294002, the bpV-mediated increase in p-Akt at 30 min was significantly inhibited (86% decrease, Fig. 3A, $p < 0.001$). Downstream mTOR activity enhanced by bpV was also reduced (86% decrease), as measured by p-S6 activity following PI3K inhibition (Fig. 3B, $p < 0.01$). Combined with rapamycin treatment, bpV-associated increase in S6 activity was also diminished in injured neurons (Fig. 3B).

Injury- and bpV- induced Erk activity was inhibited by rapamycin

As expected, bpV significantly decreased LDH release from injury ($p < 0.05$), and LDH was also significantly less than scratch + U0126 treatment (Fig. 4A, $p < 0.05$). When bpV and U0126 were combined, the LDH release was significantly decreased compared with the scratch injury ($p < 0.05$) and the scratch + U0126 ($p < 0.05$), reaching LDH levels near those observed after bpV treatment alone. The scratch injury increased and rapamycin reduced Erk activity (Fig. 4B).
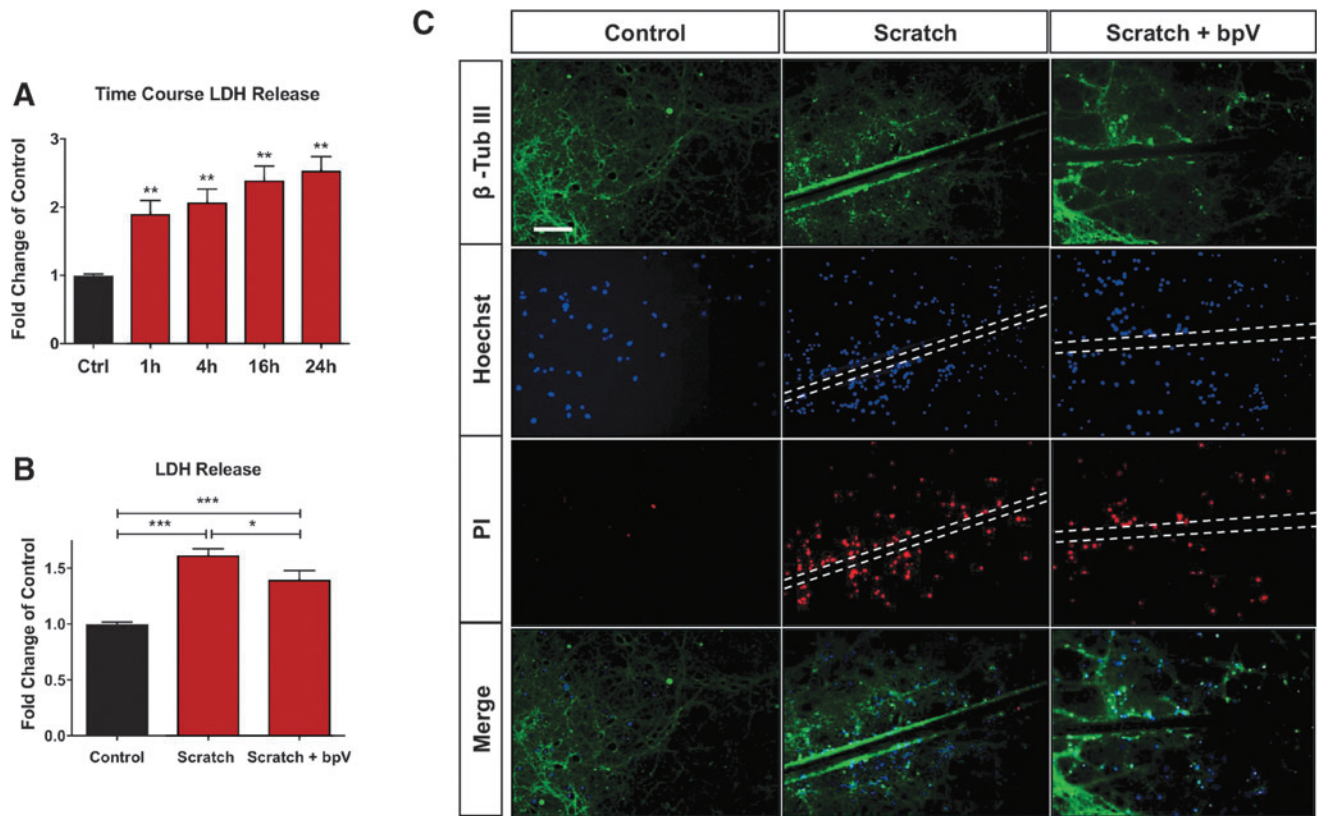
FIG. 2. BpV protected spinal neurons from injury in an *in vitro* model of trauma. (**A**) Scratch injury produced a graded increase of cell death as indicated by lactase dehydrogenase (LDH) assay ($p < 0.01$ compared with control). (**B**) Administration of 100 nM bisperoxovanadium (bpV) significantly reduced LDH release at day one post-scratch injury. (**C**) This same dose of bpV reduced propidium iodide (PI, red) and Hoechst (blue) nuclear co-labeling at 24 h in spinal neurons after scratch injury, indicating reduced cell death after the bpV treatment. Data were expressed as mean ± standard error of the mean; $n = 3$ experiments; All data analyzed via one-way analysis of variance; *$p < 0.05$; **$p < 0.01$; ***$p < 0.001$.
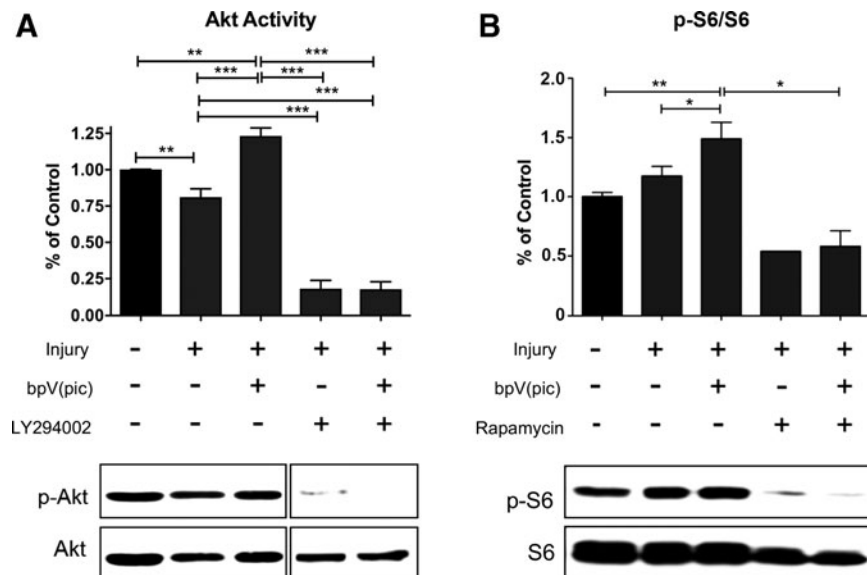

FIG. 3. Bisperoxovanadium (bpV) activated prosurvival kinase/mammalian target of rapamycin (Akt/mTOR) in injured spinal neurons *in vitro*. (**A**) Scratch injury induced a decrease in Akt phosphorylation that was significantly reversed by bpV treatment. Application of a PI3K inhibitor LY294002 diminished Akt phosphorylation in the presence of bpV. (**B**) Ribosomal protein S6 phosphorylation, a marker of mTOR activity, significantly increased after scratch injury as observed *in vivo*. Treatment with bpV significantly increased p-S6 expression over scratch-induced injury alone. Treatment with an mTOR inhibitor, rapamycin, reduced S6 phosphorylation post-scratch injury and bpV treatment. Data were expressed as mean ± standard error of the mean; $n = 3$–4 experiments; All data analyzed via one-way analysis of variance; *$p < 0.05$; **$p < 0.01$; ***$p < 0.001$.
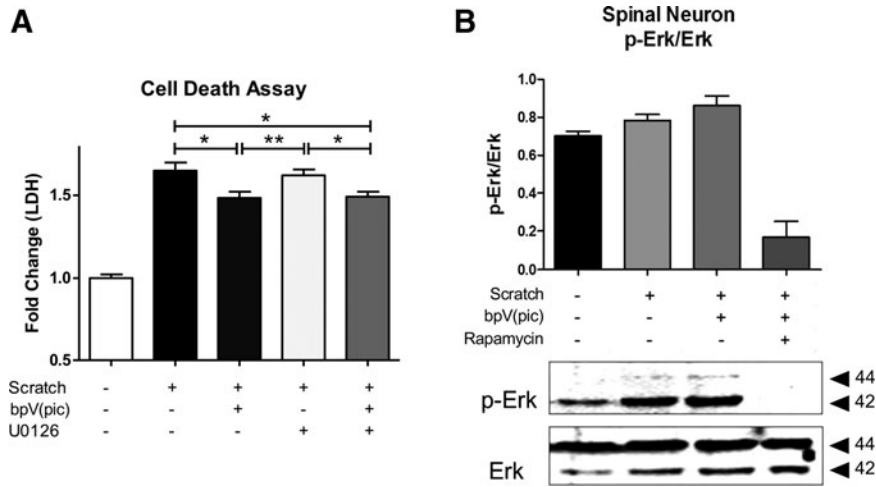
2680

FIG. 4. Bisperoxovanadium (bpV) promoted extracellular signal-related kinase (Erk) activity in an mammalian target of rapamycin (mTOR)-dependent manner. (**A**) MEK and Erk activity inhibitor, U0126, did not significantly reduce neuron scratch injury-mediated cell death, while bpV did even when combined with U0126. (**B**) Rapamycin reduced Erk activity, suggesting that the injury induced Erk activation occurred via an mTOR-dependent manner. Data were expressed as mean ± standard error of the mean; $n = 3$ experiments. All data analyzed via one-way analysis of variance; $*p < 0.05$; $**p < 0.01$; $***p < 0.001$.
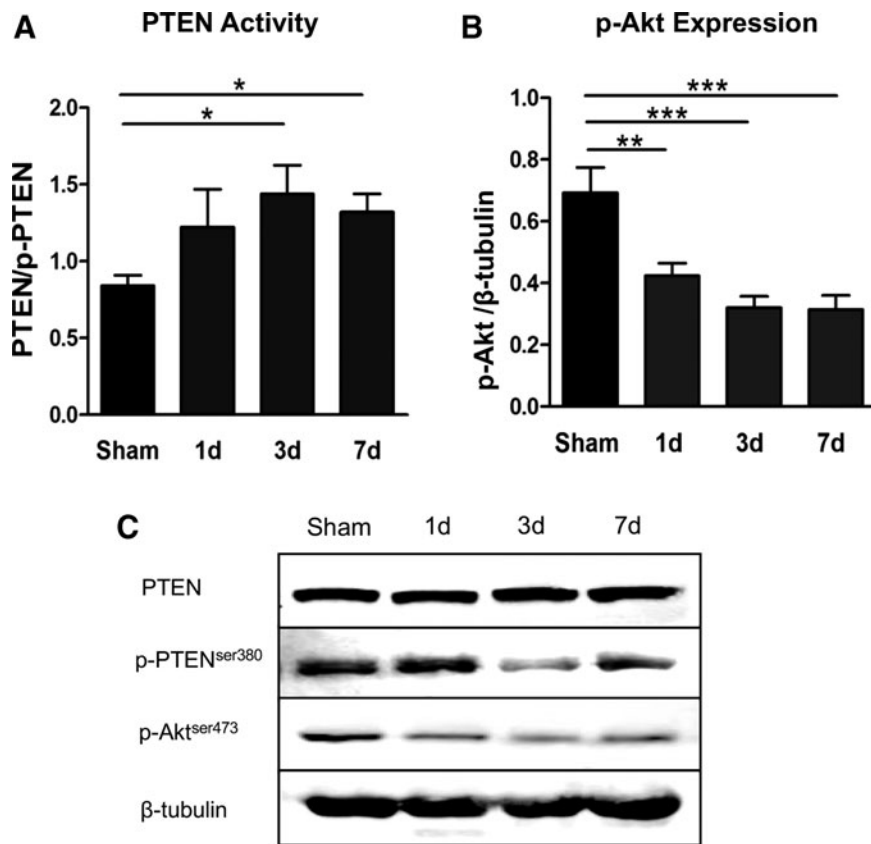

FIG. 5. Inverse relationship between phosphatase and tensin homologue (PTEN) activity and prosurvival kinase (p-Akt) expression after a cervical hemi-contusion spinal cord injury (SCI). (**A**) The PTEN phosphorylation was considerably reduced by day three post-SCI, indicating PTEN phosphatase activity increased over this period. (**B**) Conversely, Akt phosphorylation significantly decreased starting at day one post-SCI. (**C**) Representative Western blots of PTEN, p-PTEN, p-Akt, and Akt. β-tubulin served as a loading control. Data were expressed as mean ± standard error of the mean; $n = 4$–5/time point; All data analyzed via one-way analysis of variance; $*p < 0.05$; $**p < 0.01$; $***p < 0.001$.

Changes in PTEN and p-Akt expression/activation after SCI

Supporting the above described *in vitro* observations, overall PTEN expression did not change significantly in the injured spinal tissue after cervical SCI; however, PTEN activity level, depicted as a ratio of total PTEN to phospho-PTEN[ser380], significantly increased by days three and seven post-injury (3 d, 71.4% increase; 7 d, 57.1% over sham; $p < 0.05$) (Fig. 5A,C). Also corroborating our previous data, Akt phosphorylation decreased significantly by day one (39.1% decrease, $p < 0.01$) and maintained a low expression pattern throughout the first week (Fig. 5B,C).

This trend was mirrored in spinal neurons located in the ventral horn of cervical hemicontused rats (dashed box in 6A, ~ 1.5 mm distal to the injury epicenter). NeuN (green) and p-Akt (red) co-labeled ventral horn neurons showed a decrease in p-Akt expression in surviving ventral horn neurons over time after SCI.

Sham animals exhibited high levels of p-Akt in spinal motor neurons (Fig. 6B,D); however, in SCI animals, expression decreased considerably and declined significantly by seven days post-injury (Fig. 6B, $p < 0.05$) as shown through immunofluorescence double-labeling of p-Akt with neuronal marker NeuN (white

arrows) in surviving neurons ~ 1.5 mm distal to the epicenter (Fig. 6D). Neuron survival in the penumbral region of the cord, as indicated by NeuN[+] labeling, significantly decreased by day one post-SCI ($p < 0.01$), although remained similar throughout the seven day assessment period (Fig. 6C).

Injury increased Erk and S6 phosphorylation simultaneously in ventral horn neurons after SCI

Our previous studies showed bpV promoted neuroprotection of ventral horn motor neurons after C5 hemicontusion SCI.[11,12,29] Previous findings and the present study demonstrated the ability for bpV to increase S6 phosphorylation in spinal neurons both *in vivo* and *in vitro*. Further analysis of S6 phosphorylation through the first week post-SCI showed sustained elevation of p-S6 induced by injury through day seven post-SCI (Fig. 7H,I). Likewise, Erk phosphorylation and activity was also increased at one d post-injury and remained high throughout this period (Fig. 7G,I) compared with the sham group (Fig. 7G). This increase occurred simultaneously in the same population of neurons as demonstrated at one day post-SCI compared with the sham group (Fig. 7A–F).
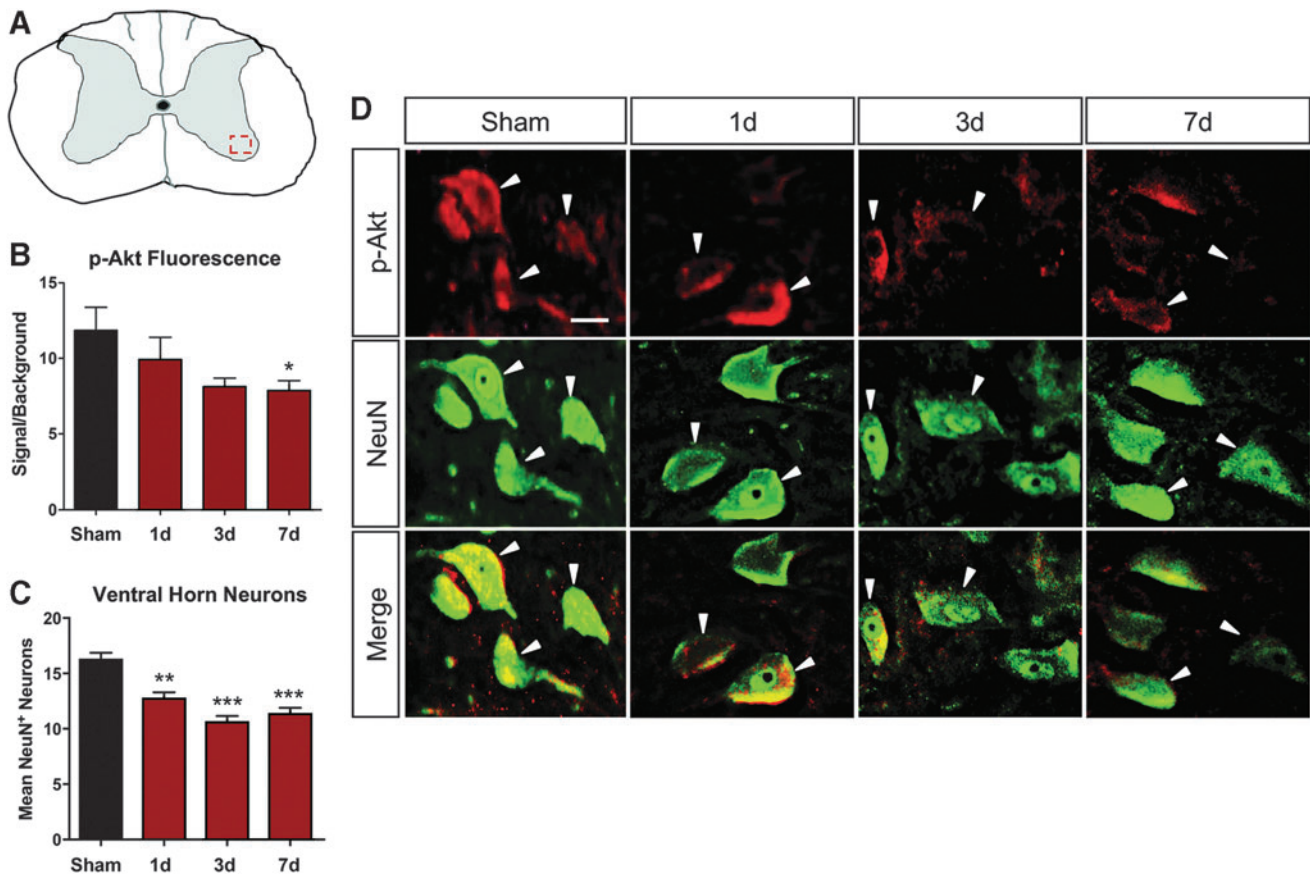

FIG. 6. Ventral horn motor neuron prosurvival kinase (p-Akt) expression mirrored total spinal tissue p-Akt expression post-spinal cord injury (SCI). **(A)** Illustration of region of neuronal imaging and quantification. **(B)** As shown for total spinal tissue, Akt phosphorylation decreased in ventral horn neurons throughout the first week post-SCI. **(C)** Ventral horn neurons were significantly decreased in the penumbral region beginning one day post-injury, but sustained this level throughout the first week after SCI. **(D)** Representative double immunofluorescence labeling shows decreased Akt phosphorylation in the ventral horn motor neurons over time post-injury. Data were expressed as mean ± standard error of the mean; $n = 3$/ time point; All data analyzed via one-way analysis of variance; *$p < 0.05$ compared with sham.
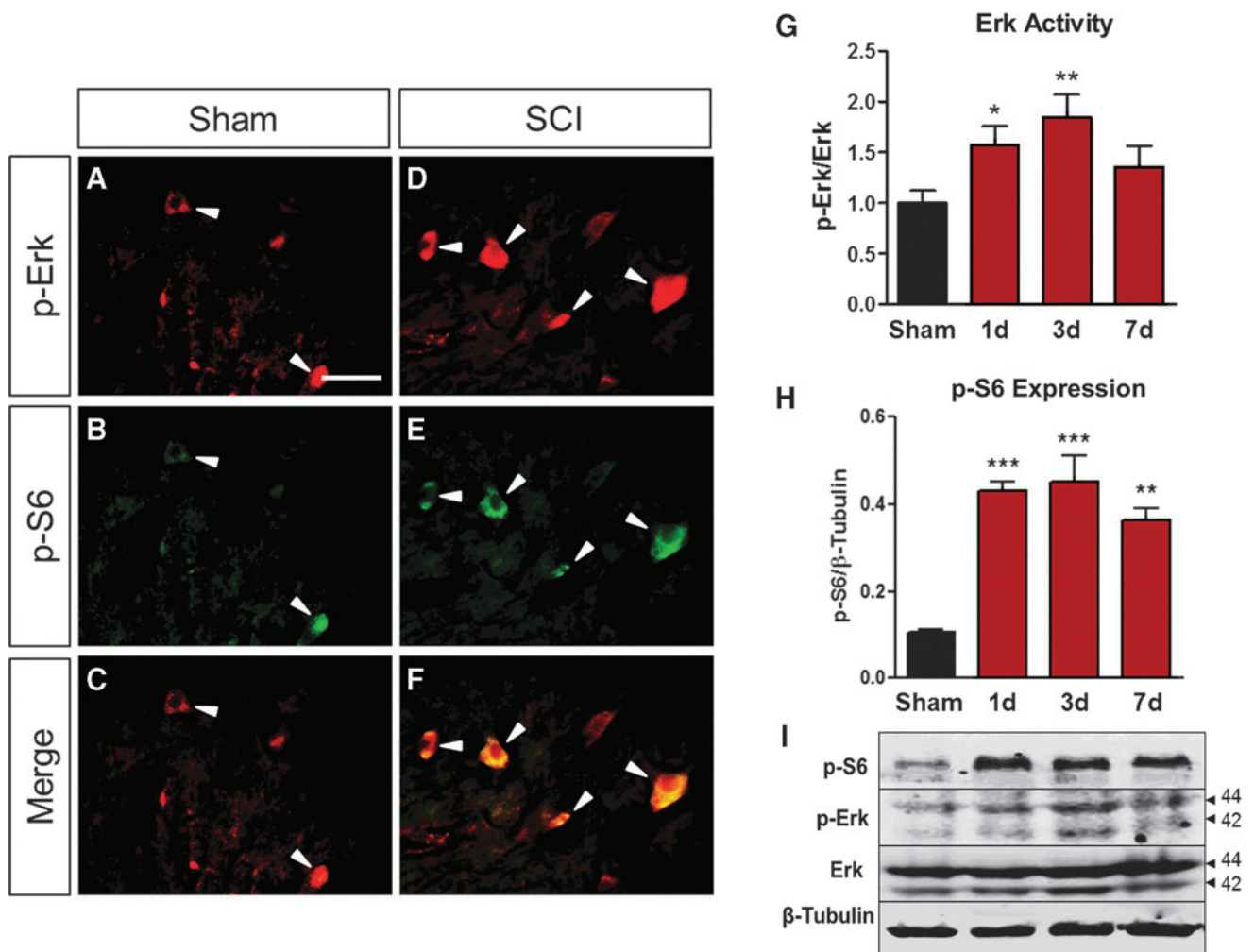
FIG. 7. Extracellular signal-related kinase (Erk) and p-S6 colocalized and showed similar expression profile in the spinal cord after injury. **(A–F)** Both p-Erk and p-S6 were highly expressed in the ventral horn motor neurons at 24 h post-SCI compared with the sham control (white arrows). (G,I) The Erk activity and (H,I) p-S6 showed similarly expressional changes over time in the total spinal cord tissue. (I) Representative Western blot images for p-S6, p-Erk, and Erk. β-tubulin served as a loading control. Data were expressed as mean ± standard error of the mean; $n = 3$ for immunofluorescence double labeling. $n = 4$–5/time point for Western blot. All data analyzed via one-way analysis of variance; $n = 3$ for immunofluorescence double labeling. $n = 4$–5/ time point for Western blot. $*p < 0.05$; $**p < 0.01$; $***p < 0.001$ compared with sham.

Treatment with bpV decreased caspase 3 activity and increased GSK3β phosphorylation and Erk activity after SCI

In assessment of bpV effects on apoptotic cell death, caspase 3 activity was assessed through Western blot one day after injury. The SCI significantly increased caspase 3 activity (67.1%) at this time point ($p < 0.01$ vs. sham), and treatment with saline vehicle did not influence injury-mediated caspase 3 activity (Fig. 8A,D). Treatment with bpV significantly reduced caspase 3 activity at one day post-SCI (27.3%) ($p < 0.05$) to approximate levels observed in sham animals.

To support the hypothesis that bpV increased Akt activity, because GSK3β is directly phosphorylated by Akt,[30] GSK3β at serine 9 was examined. Treatment with bpV increased GSK3β phosphorylation at this residue over endogenous levels by one day after SCI (Fig. 8B,D). During this same period, bpV significantly elevated injury-mediated phosphorylation and activation of Erk (Fig. 8C,D, $p < 0.01$).

Discussion

Multiple nervous system disease and injury studies implicated neuroprotective and cellular mechanisms of bpV effects.[7,17,31–34] The present study has provided new evidence of the protective effect of bpV on injured spinal neurons *in vitro* and *in vivo,* and revealed a mechanism of the action of bpV on PI3K/Akt-mTOR axis signaling in neurons (Fig. 9). Because both Akt activation and bpV administration have been demonstrated widely to have survival-enhancing effects, further studies aimed at translating these strategies, alone or in combination, are warranted.

In addition, our findings support the notion that bpV could also activate the Erk signaling pathway.[35] The direct role of this MAPK pathway in bpV-mediated protection in the present study remains unclear, but appears limited. Understanding how bpV promotes neuron survival and its molecular mechanisms, as presented in this study, in both *in vitro* and *in vivo* trauma models, should be useful for further investigation aimed at improving functional outcomes after SCI.
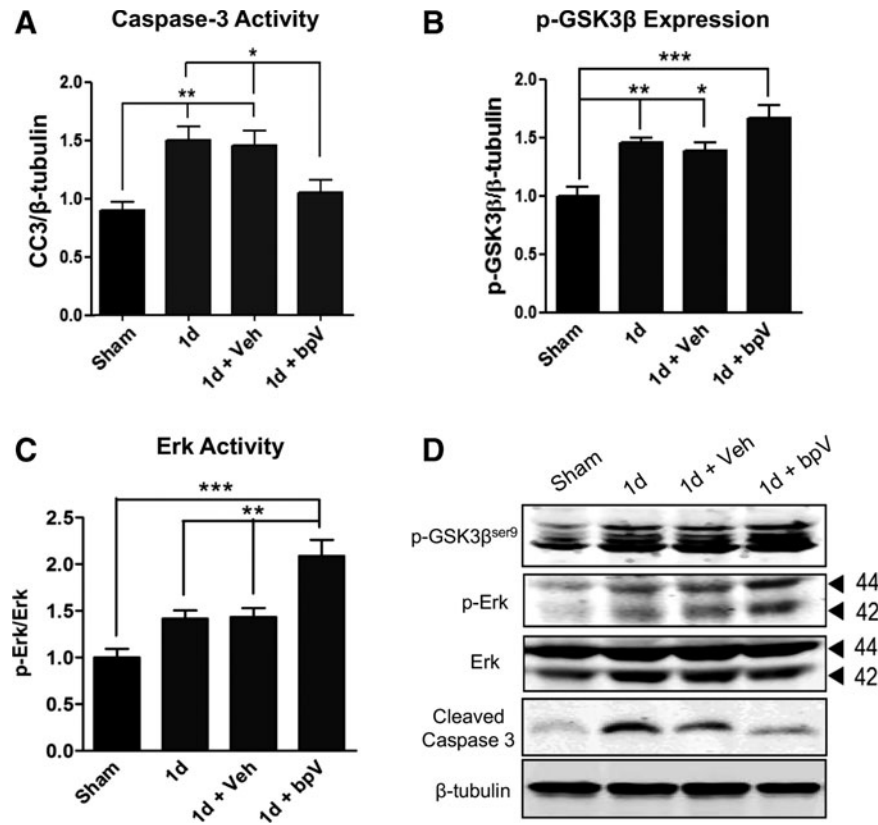
FIG. 8. Bisperoxovanadium (bpV) reduced apoptosis, and enhanced extracellular signal-related kinase (Erk) and glycogen synthase kinase (GSK) 3β activation after spinal cord injury (SCI). (**A**) Treatment with bpV significantly decreased SCI-induced elevation in caspase 3 activity at one day post-injury. Simultaneously, (**B**) GSK3β phosphorylation, a marker of Akt activity, and (**C**) Erk activity were increased by bpV in injured spinal tissue. (**D**) Representative Western blots of p-GSK3β, cleaved caspase 3, p-Erk, and Erk. β-tubulin served as a loading control. Data were expressed as mean $\pm$ standard error of the mean; $n = 4$–6 for Western blot. All data analyzed via one-way analysis of variance; $*p < 0.05$; $**p < 0.01$; $***p < 0.001$.
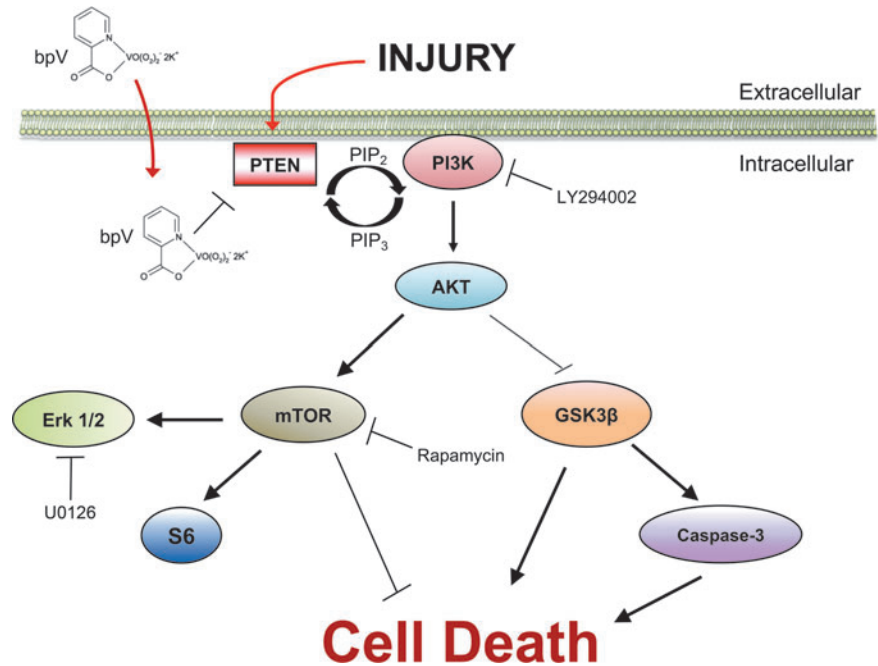

FIG. 9. Schematic diagram for proposed mechanisms of injury and bisperoxovanadium (bpV)-induced signaling changes *in vivo* and *in vitro*. Based on our findings, we believe bpV-mediated neuroprotection in spinal cord injury and an *in vitro* model of spinal neuron injury primarily through PI3K/Akt/mTOR signaling. The activation of extracellular signal-related kinase (Erk) also appears to play a role, although this appears to be mediated through cross-talk with mTOR. Akt/mTOR, prosurvival kinase/mammalian target of rapamycin; PTEN, phosphatase and tensin homologue.

Treatment with bpV activated Akt/mTOR signaling in spinal neurons after traumatic insults

With a pre-treatment of 100 nM bpV, Akt activity was significantly increased over the injury-only control and non-injured control (Fig. 3A, $p < 0.001$) suggesting bpV was acting through inhibition of PTEN, promoting PI3K activity and subsequent Akt phosphorylation. We observed a similar result in Akt activity upregulation *in vivo* after SCI and bpV treatment.[11] In that *in vivo* study, ribosomal protein S6 activation, as measured through phosphorylation of S6 at ser 235/236, was observed in both total tissue protein analysis and neuron immunofluorescence labeling. In the present study, S6 phosphorylation and activation also increased after bpV treatment (Fig. 3B), indicating the activation of mTOR, which is often determined by observing or quantifying p-S6.[7,9,11,36]

As such, we proposed that bpV acted through this axis by disinhibiting PI3K and promoting downstream mTOR activity. Application of the PI3K inhibitor LY294002 significantly reduced the activity of Akt (Fig. 3A, $p < 0.001$) and decreased S6 phosphorylation (Fig. 3B) after injury and bpV pre-treatment, supporting our expectations that we expected trauma and bpV-mediated effects on mTOR activity would be diminished after PI3K inhibition if mTOR was regulated directly by PI3K signaling after injury.

Because Akt activity was greatly reduced after LY294002 application, despite bpV treatment, our results support our hypothesis that the effect of bpV is mediated through PTEN inhibition and activation of Akt/mTOR signaling axis after SCI. This conclusion was supported further by the considerable downregulation of bpV-stimulated p-S6 increase through rapamycin treatment (Fig. 3B). This evidence is in accordance with our previous findings showing that bpV upregulated mTOR activity and S6 phosphorylation in the penumbral spinal cord tissue after injury.[11]

Akt phosphorylation and PTEN activity were inversely proportional after SCI

Yu and associates[37] demonstrated that neurons in the penumbral region upregulated Akt phosphorylation by 8 h after SCI and rapidly downregulated by 24 h post-injury. In the present study, we showed that penumbral neurons downregulated p-Akt by one day after cervical contusion injury, a pattern that continued throughout the first week after SCI. The similar neuronal Akt phosphorylation response pattern and the whole spinal tissue downregulation of p-Akt suggests that neurons may be the primary cells influencing Akt activity after SCI. Brief inspection of Akt phosphorylation in glial cells in the region of the studied neurons was not conclusive; however, additional research is being performed to further assess the signaling changes in glia after injury and bpV treatment.

Although Yu and colleagues[37] examined motor neurons 3–6 mm distal to the injury site and we examined such cells approximately 1.5 mm from the epicenter, the overall trend is comparable. The neurons we examined survived initial necrotic death within the gray matter adjacent to the epicenter of injury during the first day post-SCI.[38] Because of their proximity to this region, these neurons were affected directly by the spread of secondary damage to tissue and adjacent cells, which might have altered their response and health over time after injury.

Our results suggest that spinal neuron downregulation of Akt phosphorylation correlates well with the time course of apparent increase in PTEN activity as measured through the ratio of PTEN (active) to p-PTEN (inactive) (Fig. 5). These results support our previous findings[11] and support the use of Akt phosphorylation as a marker of PTEN activity. As such, our expectation that bpV was

acting through PTEN was confirmed further by these results, as well as the increase in phosphorylation of GSK3β, a downstream effector of Akt,[30] after bpV treatment (Fig. 8). This is in agreement with our previous finding that bpV increased phosphorylation of ribosomal protein S6, a marker for mTOR activity, *in vivo*.[11]

Treatment with bpV inhibited PTEN activation and reduced cell death after injury in vivo *and* in vitro

The correlation of PTEN activity with elevated neuronal death was supported by the observed increase in caspase-3 activity at one day after SCI. Alternatively, the neuroprotective effects of bpV were reinforced by significantly reducing caspase 3 activity at this time point (Fig. 8). Interestingly, the pattern of SCI-induced elevation in autophagosome formation[11,39–41] and caspase 3 activity and the reduction of bpV in these activities are quite similar. It remains unclear whether or not increased autophagosome aggregation after SCI is neuroprotective[42]; however, this result supported bpV as a protective agent for neurons under traumatic conditions.

To determine the effect of bpV on spinal neurons after trauma, we augmented a neuronal scratch injury model (Fig. S1) previously used to study traumatic brain injury in primary cortical neurons[21] and applied it to our established spinal neuron culture.[20] We confirmed bpV is protective in spinal neurons after traumatic scratch injury. We then hypothesized that traumatic injury *in vitro* would also affect PTEN and PI3K signaling resulting in a reduction in Akt phosphorylation and activity, replicating our observations *in vivo*. An acute pattern of signaling changes was observed, and spinal neurons significantly downregulated Akt activity ($p < 0.05$; Fig. 3).

Treatment with bpV increased Erk activity in an mTOR-dependent manner

We have provided evidence that bpV upregulated Erk signaling here and in supplemental experiments (Supplementary Fig. S2), and that blocking mTOR via rapamycin reduced this increase in Erk activity. This is intriguing because it suggests two different pathways may be modulated by bpV in injured spinal neurons. Erk 1/2 signaling previously has been shown to play a neuroprotective role in neurological injury and disease[43]; however, the effects of bpV compounds on Erk signaling has only been investigated recently.

A recent study indicates that Erk activation plays a primary role in bpV-mediated neuroprotection in a rodent model of cerebral ischemia-reperfusion injury,[33] and a newly synthesized bpV molecule, bisperoxovandium (pyridin-2-squaramide), has been shown to promote neuroprotection in ischemia-reperfusion injury through upregulation of both Akt and Erk 1/2 activity.[44] In light of these findings, it is possible that Erk1/2 upregulation by bpV has a neuroprotective influence in our study.

Although it is possible that bpV could act as a protein tyrosine phosphatase upstream of MAPK-MEK to contribute to the observed effects, the results presented here suggest that Erk activation mediated by bpV occurs through cross-talk in an mTOR-dependent manner. Inhibiting MEK upstream of Erk via U0126 did not significantly change scratch injury-induced cell damage/death and bpV mediated significant reduction in such pathology despite administration of U0126. Therefore, although bpV upregulates Erk activity, the neuroprotection afforded by bpV treatment appears to occur primarily through the PI3K/Akt-mTOR axis.

Pleiotropic functions of mTOR are well documented, with its effects being cell and context dependent.[45] Rapamycin has been shown to promote autophagy as well as induce apoptosis,[45] and

there is still debate over whether autophagy positively or negatively influences neuronal survival and pathological outcome after traumatic SCI and neuronal damage.[11,42,46,47] Likewise, Erk activity has also been linked to both positive and negative outcomes post-SCI.[48–50]

In our study, the treatment of damaged spinal neurons with U0126 did not impact cell health negatively. On the contrary, U0126 significantly decreased cell damage in combination with bpV as measured through LDH release (Fig. 4A). We did not, however, specifically examine the autophagic or apoptotic impact of rapamycin treatment in our *in vitro* experiments. Rapamycin administration correlated with a reduction in Erk activity, while bpV stimulated its activity; this raises interesting questions about the involvement of Erk in the neuroprotective responses obtained through bpV-mediated upregulation of PI3K/Akt-mTOR signaling.

Acute upregulation of Erk activity in ventral horn neurons *in vivo* corresponded with a simultaneous upregulation of ribosomal protein S6 phosphorylation (Fig. 7), which supports our *in vitro* findings linking mTOR and Erk activity. It must be considered, however, that mTOR may be regulating both pathways for separate purposes. Nevertheless, the overall outcome is positive, likely because of primary effects on Akt-mTOR survival signaling. Further examination of the autophagy or apoptotic response would shed light on the involvement of these processes in the results observed in the present study.

Conclusions

Understanding cellular responses to traumatic insult is challenging, because intracellular protein interactions and activation of multiple signaling cascades complicate experimental interpretation. At the tissue level, SCI causes disruption of axon tracts and immediate local cell death and triggers delayed spread of damage and a glial response that chronically inhibits axonal regeneration.

In the present study, we demonstrated that the bpV compound has a protective effect on neurons in both *in vitro* and *in vivo* models of traumatic spinal injury and that such an effect is mediated through the inhibition of PTEN and activation of PI3K/AKT–mTOR signal pathway. The bpV compounds have been shown to be protective or regenerative through p-Akt signaling in cortical neurons in other injury models.[14,32,51]

To our knowledge, this study is the first to demonstrate the effect of bpV on spinal neuronal survival and PTEN/PI3K signaling after traumatic spinal injury *in vivo* and *in vitro*. Also, our results show that bpV stimulates mTOR activity, suggesting bpV could potentially promote spinal neuron axonal regeneration. Future studies will further dissect the mechanism of action of bpV on neuroprotection and regeneration in spinal neurons, explore its effects on other cells such as glial cells, and examine its effects on promoting recovery of function in disease models such as traumatic spinal cord and brain injuries.

Acknowledgments

Author Disclosure Statement

No competing financial interests exist.

Supplementary Material

Supplementary Figure S1
Supplementary Figure S2

References

1. Ackery, A., Tator, C., and Krassioukov, A. (2004). A global perspective on spinal cord injury epidemiology. J. Neurotrauma 21, 1355–1370.
2. Kirshblum, S.C., Groah, S.L., McKinley, W.O., Gittler, M.S., and Stiens, S.A. (2002). Spinal cord injury medicine. 1. Etiology, classification, and acute medical management. Arch. Phys. Med. Rehabil. 83, Suppl 1, S50–S57.
3. Kirshblum, S.C. (2002). Clinical activities of the model spinal cord injury system. J. Spinal Cord Med. 25, 339–344.
4. Varma, A.K., Das, A., Wallace, G., 4th, Barry, J., Vertegel, A.A., Ray, S.K., and Banik, N.L. (2013). Spinal cord injury: a review of current therapy, future treatments, and basic science frontiers. Neurochem. Res. 38, 895–905.
5. Nandoe Tewarie, R.D., Hurtado, A., Bartels, R.H., Grotenhuis, J.A., and Oudega, M. (2010). A clinical perspective of spinal cord injury. NeuroRehabilitation 27, 129–139.
6. Lewandowski, G. and Steward, O. (2014). AAVshRNA-mediated suppression of PTEN in adult rats in combination with salmon fibrin administration enables regenerative growth of corticospinal axons and enhances recovery of voluntary motor function after cervical spinal cord injury. J. Neurosci. 34, 9951–9962.
7. Liu, K., Lu, Y., Lee, J.K., Samara, R., Willenberg, R., Sears-Kraxberger, I., Tedeschi, A., Park, K.K., Jin, D., Cai, B., Xu, B., Connolly, L., Steward, O., Zheng, B., and He, Z. (2010). PTEN deletion enhances the regenerative ability of adult corticospinal neurons. Nat. Neurosci. 13, 1075–1081.
8. Park, J.H., Lee, J.Y., Shin, D.H., Jang, K.S., Kim, H.J., and Kong, G. (2011). Loss of Mel-18 induces tumor angiogenesis through enhancing the activity and expression of HIF-1alpha mediated by the PTEN/PI3K/Akt pathway. Oncogene 39, 4578–4589.
9. Sun, F., Park, K.K., Belin, S., Wang, D., Lu, T., Chen, G., Zhang, K., Yeung, C., Feng, G., Yankner, B.A., and He, Z. (2011). Sustained axon regeneration induced by co-deletion of PTEN and SOCS3. Nature 480, 372–375.
10. Ohtake, Y., Park, D., Abdul-Muneer, P.M., Li, H., Xu, B., Sharma, K., Smith, G.M., Selzer, M.E., and Li, S. (2014). The effect of systemic PTEN antagonist peptides on axon growth and functional recovery after spinal cord injury. Biomaterials 35, 4610–4626.
11. Walker, C.L., Walker, M.J., Liu, N.K., Risberg, E.C., Gao, X., Chen, J., and Xu, X.M. (2012). Systemic bisperoxovanadium activates Akt/mTOR, reduces autophagy, and enhances recovery following cervical spinal cord injury. PLoS One 7, e30012.
12. Walker, C.L. and Xu, X.M. (2014). PTEN inhibitor bisperoxovanadium protects oligodendrocytes and myelin and prevents neuronal atrophy in adult rats following cervical hemicontusive spinal cord injury. Neurosci. Lett. 573, 64–68.
13. Li, D., Qu, Y., Mao, M., Zhang, X., Li, J., Ferriero, D., and Mu, D. (2009). Involvement of the PTEN-AKT-FOXO3a pathway in neuronal apoptosis in developing rat brain after hypoxia-ischemia. J. Cereb. Blood Flow Metab. 29, 1903–1913.
14. Ding, J., Guo, J., Yuan, Q., Yuan, F., Chen, H., and Tian, H. (2013). Inhibition of phosphatase and tensin homolog deleted on chromosome 10 decreases rat cortical neuron injury and blood-brain barrier permeability, and improves neurological functional recovery in traumatic brain injury model. PLoS One 8, e80429.
15. Shi, G.D., OuYang, Y.P., Shi, J.G., Liu, Y., Yuan, W., and Jia, L.S. (2011). PTEN deletion prevents ischemic brain injury by activating the mTOR signaling pathway. Biochem. Biophys. Res. Commun. 404, 941–945.
16. Zhang, Q.G., Wu, D.N., Han, D. and Zhang, G.Y. (2007). Critical role of PTEN in the coupling between PI3K/Akt and JNK1/2 signaling in ischemic brain injury. FEBS Lett. 581, 495–505.
17. Sury, M.D., Vorlet-Fawer, L., Agarinis, C., Yousefi, S., Grandgirard, D., Leib, S.L., and Christen, S. (2011). Restoration of Akt activity by the bisperoxovanadium compound bpV(pic) attenuates hippocampal

apoptosis in experimental neonatal pneumococcal meningitis. Neurobiol. Dis. 41, 201–208.

18. Song, W., Volosin, M., Cragnolini, A.B., Hempstead, B.L. and Friedman, W.J. (2010). ProNGF induces PTEN via p75NTR to suppress Trk-mediated survival signaling in brain neurons. J. Neurosci. 30, 15608–15615.

19. Schmid, A.C., Byrne, R.D., Vilar, R., and Woscholski, R. (2004). Bisperoxovanadium compounds are potent PTEN inhibitors. FEBS Lett. 566, 35–38.

20. Jiang, X.Y., Fu, S.L., Nie, B.M., Li, Y., Lin, L., Yin, L., Wang, Y.X., Lu, P.H., and Xu, X.M. (2006). Methods for isolating highly-enriched embryonic spinal cord neurons: a comparison between enzymatic and mechanical dissociations. J. Neurosci. Methods 158, 13–18.

21. Zhao, Y., Luo, P., Guo, Q., Li, S., Zhang, L., Zhao, M., Xu, H., Yang, Y., Poon, W., and Fei, Z. (2012). Interactions between SIRT1 and MAPK/ERK regulate neuronal apoptosis induced by traumatic brain injury in vitro and in vivo. Exp. Neurol. 237, 489–498.

22. Wu, X., Walker, C.L., Lu, Q., Wu, W., Eddelman, D.B., Parish, J.M., and Xu, X.M. (2017). RhoA/Rho kinase mediates neuronal death through regulating cPLA$_2$ activation. Mol. Neurobiol. 54, 6885–6895.

23. Liu, N.K., Zhang, Y.P., Titsworth, W.L., Jiang, X., Han, S., Lu, P.H., Shields, C.B., and Xu, X.M. (2006). A novel role of phospholipase A2 in mediating spinal cord secondary injury. Ann. Neurol. 59, 606–619.

24. Bradford, M.M. (1976). A rapid and sensitive method for the quantitation of microgram quantities of protein utilizing the principle of protein-dye binding. Anal. Biochem. 72, 248–254.

25. Walker, M.J., Walker, C.L., Zhang, Y.P., Shields, L.B., Shields, C.B., and Xu, X.M. (2015). A novel vertebral stabilization method for producing contusive spinal cord injury. J. Vis. Exp. e50149.

26. Gruner, J.A. (1992). A monitored contusion model of spinal cord injury in the rat. J. Neurotrauma 9, 123–126.

27. Gensel, J.C., Tovar, C.A., Hamers, F.P., Deibert, R.J., Beattie, M.S., and Bresnahan, J.C. (2006). Behavioral and histological characterization of unilateral cervical spinal cord contusion injury in rats. J. Neurotrauma 23, 36–54.

28. Deng, L.X., Hu, J., Liu, N., Wang, X., Smith, G.M., Wen, X., and Xu, X.M. (2011). GDNF modifies reactive astrogliosis allowing robust axonal regeneration through Schwann cell-seeded guidance channels after spinal cord injury. Exp. Neurol. 229, 238–250.

29. Walker, C.L., Wang, X., Bullis, C., Liu, N.K., Lu, Q., Fry, C., Deng, L., and Xu, X.M. (2015). Biphasic bisperoxovanadium administration and Schwann cell transplantation for repair after cervical contusive spinal cord injury. Exp. Neurol. 264, 163–172.

30. Cross, D.A., Alessi, D.R., Cohen, P., Andjelkovich, M., and Hemmings, B.A. (1995). Inhibition of glycogen synthase kinase-3 by insulin mediated by protein kinase B. Nature 378, 785–789.

31. Nakashima, S., Arnold, S.A., Mahoney, E.T., Sithu, S.D., Zhang, Y.P., D'Souza, S.E., Shields, C.B., and Hagg, T. (2008). Small-molecule protein tyrosine phosphatase inhibition as a neuroprotective treatment after spinal cord injury in adult rats. J. Neurosci. 28, 7293–7303.

32. Mao, L., Jia, J., Zhou, X., Xiao, Y., Wang, Y., Mao, X., Zhen, X., Guan, Y., Alkayed, N.J., and Cheng, J. (2013). Delayed administration of a PTEN inhibitor BPV improves functional recovery after experimental stroke. Neuroscience 231, 272–281.

33. Liu, R., Tang, J.C., Pan, M.X., Zhuang, Y., Zhang, Y., Liao, H.B., Zhao, D., Lei, Y., Lei, R.X., Wang, S., Liu, A.C., Qin, X.P., Chen, J., Zhang, Z.F., and Wan, Q. (2018). ERK 1/2 activation mediates the neuroprotective effect of BpV(pic) in focal cerebral ischemia-reperfusion injury. Neurochem. Res. 43, 1424–1438.

34. Mao, L.L., Hao, D.L., Mao, X.W., Xu, Y.F., Huang, T.T., Wu, B.N., and Wang, L.H. (2015). Neuroprotective effects of bisperoxovanadium on cerebral ischemia by inflammation inhibition. Neurosci. Lett. 602, 120–125.

35. De Paula, M.L., Cui, Q.L., Hossain, S., Antel, J., and Almazan, G. (2014). The PTEN inhibitor bisperoxovanadium enhances myelination by amplifying IGF-1 signaling in rat and human oligodendrocyte progenitors. Glia 62, 64–77.

36. Park, K.K., Liu, K., Hu, Y., Smith, P.D., Wang, C., Cai, B., Xu, B., Connolly, L., Kramvis, I., Sahin, M., and He, Z. (2008). Promoting axon regeneration in the adult CNS by modulation of the PTEN/mTOR pathway. Science 322, 963–966.

37. Yu, F., Sugawara, T., Maier, C.M., Hsieh, L.B., and Chan, P.H. (2005). Akt/Bad signaling and motor neuron survival after spinal cord injury. Neurobiol. Dis. 20, 491–499.

38. Ek, C.J., Habgood, M.D., Callaway, J.K., Dennis, R., Dziegielewska, K.M., Johansson, P.A., Potter, A., Wheaton, B., and Saunders, N.R. (2010). Spatio-temporal progression of grey and white matter damage following contusion injury in rat spinal cord. PLoS One 5, e12021.

39. Kanno, H., Ozawa, H., Sekiguchi, A., and Itoi, E. (2009). Spinal cord injury induces upregulation of Beclin 1 and promotes autophagic cell death. Neurobiol. Dis. 33, 143–148.

40. Kanno, H., Ozawa, H., Sekiguchi, A., Yamaya, S., and Itoi, E. (2011). Induction of autophagy and autophagic cell death in damaged neural tissue after acute spinal cord injury in mice. Spine (Phila Pa 1976) 36, E1427–E1434.

41. Zhang, H.Y., Wang, Z.G., Wu, F.Z., Kong, X.X., Yang, J., Lin, B.B., Zhu, S.P., Lin, L., Gan, C.S., Fu, X.B., Li, X.K., Xu, H.Z., and Xiao, J. (2013). Regulation of autophagy and ubiquitinated protein accumulation by bFGF promotes functional recovery and neural protection in a rat model of spinal cord injury. Mol. Neurobiol. 48, 452–464.

42. Sekiguchi, A., Kanno, H., Ozawa, H., Yamaya, S., and Itoi, E. (2012). Rapamycin promotes autophagy and reduces neural tissue damage and locomotor impairment after spinal cord injury in mice. J. Neurotrauma 29, 946–956.

43. Walker, C.L., Liu, N.K., and Xu, X.M. (2013). PTEN/PI3K and MAPK signaling in protection and pathology following CNS injuries. Front. Biol. (Beijing) 8.

44. Zhang, Z.F., Chen, J., Han, X., Zhang, Y., Liao, H.B., Lei, R.X., Zhuang, Y., Wang, Z.F., Li, Z., Chen, J.C., Liao, W.J., Zhou, H.B., Liu, F., and Wan, Q. (2017). Bisperoxovandium (pyridin-2-squaramide) targets both PTEN and ERK1/2 to confer neuroprotection. Br. J. Pharmacol. 174, 641–656.

45. Castedo, M., Ferri, K.F., and Kroemer, G. (2002). Mammalian target of rapamycin (mTOR): pro- and anti-apoptotic. Cell Death Differ. 9, 99–100.

46. Guo, Y., Wang, F., Li, H., Liang, H., Li, Y., Gao, Z., and He, X. (2018). Metformin protects against spinal cord injury by regulating autophagy via the mTOR signaling pathway. Neurochem. Res. 43, 1111–1117.

47. Wang, Z., Zhou, L., Zheng, X., Chen, G., Pan, R., Li, J., and Liu, W. (2017). Autophagy protects against PI3K/Akt/mTOR-mediated apoptosis of spinal cord neurons after mechanical injury. Neurosci. Lett. 656, 158–164.

48. Yu, C.G., Yezierski, R.P., Joshi, A., Raza, K., Li, Y., and Geddes, J.W. (2010). Involvement of ERK2 in traumatic spinal cord injury. J. Neurochem. 113, 131–142.

49. Gao, L., Li, L.H., Xing, R.X., Ou, S., Liu, G.D., Wang, Y.P., Zhang, H., Gao, G.D., and Wang, T.H. (2012). Gastrocnemius-derived BDNF promotes motor function recovery in spinal cord transected rats. Growth Factors 30, 167–175.

50. Cruz, C.D. and Cruz, F. (2007). The ERK 1 and 2 pathway in the nervous system: from basic aspects to possible clinical applications in pain and visceral dysfunction. Curr. Neuropharmacol. 5, 244–252.

51. Zhao, J., Qu, J., Wu, J., Cao, M., Ferriero, D.M., Zhang, L., and Mu, D. (2013). PTEN inhibition prevents rat cortical neuron injury after hypoxia-ischemia. Neuroscience 238, 242–251.

Address correspondence to:
Xiao-Ming Xu, PhD
Spinal Cord and Brain Injury Research Group
Stark Neurosciences Research Institute
320 W. 15th Street, NS Building, Room 500E
Indianapolis, IN 46202

E-mail: xu26@iupui.edu